An investigation of the parameter space for a family of dissipative mappings

Juliano A. de Oliveira, Leonardo T. Montero, Diogo R. da Costa (iD), J. A. Méndez-Bermúdez (iD), Rene O. Medrano-T, and Edson D. Leonel

View Online   Export Citation   CrossMark

AIP Author Services
English Language Editing

AIP Publishing

An investigation of the parameter space for a family of dissipative mappings

Juliano A. de Oliveira,[1,2,a)] Leonardo T. Montero,[1,b)] Diogo R. da Costa,[3,c)] J. A. Méndez-Bermúdez,[4,d)] Rene O. Medrano-T,[5,e)] and Edson D. Leonel[2,f)]

AFFILIATIONS

[1]Universidade Estadual Paulista (UNESP), Câmpus de São João da Boa Vista, Av. Profa. Isette Corrêa Fontão, 505, 13876-750 SP, Brazil
[2]Departamento de Física, Universidade Estadual Paulista (UNESP), Instituto de Geociências e Ciências Exatas, Câmpus de Rio Claro, Av. 24A, 1515, 13506-900 SP, Brazil
[3]Programa de Pós-Graduação em Ciências/Física, Universidade Estadual de Ponta Grossa (UEPG), Câmpus Uvaranas, Ponta Grossa 84030-900, PR, Brazil
[4]Instituto de Física, Benemérita Universidad Autónoma de Puebla, Apartado Postal J-48, Puebla 72570, Mexico
[5]Departamento de Física, Universidade Federal de São Paulo (UNIFESP), Instituto de Ciências Ambientais, Químicas e Farmacêuticas, Câmpus de Diadema, R. São Nicolau, 210, 09913-030 SP, Brazil

[a)]**Electronic mail:** julianoantonio@gmail.com
[b)]**Electronic mail:** leonardotorresmontero@yahoo.com.br
[c)]**URL:** http://diogoricardo.wix.com/site. **Electronic mail:** diogo_cost@hotmail.com
[d)]**URL:** http://www.ifuap.buap.mx/~jmendezb/. **Electronic mail:** jmendezb@ifuap.buap.mx
[e)]**Electronic mail:** rmedranotorricos@gmail.com
[f)]**Electronic mail:** edleonel@rc.unesp.br

ABSTRACT

The parameter plane investigation for a family of two-dimensional, nonlinear, and area contracting map is made. Several dynamical features in the system such as tangent, period-doubling, pitchfork, and cusp bifurcations were found and discussed together with cascades of period-adding, period-doubling, and the Feigenbaum scenario. The presence of spring and saddle-area structures allow us to conclude that cubic homoclinic tangencies are present in the system. A set of complex sets such as streets with the same periodicity and the period-adding of spring-areas are observed in the parameter space of the mapping.

Published under license by AIP Publishing. https://doi.org/10.1063/1.5048513

In this paper, we consider the two-dimensional dissipative nonlinear map[1]

$$T : \begin{cases} I_{n+1} = |\delta I_n - (1+\delta)\epsilon \sin(2\pi\theta_n)|, \\ \theta_{n+1} = \theta_n + I_{n+1}^{\gamma} \qquad \text{mod}(1), \end{cases} \quad (1)$$

where I and θ are the two dynamical variables. The parameter ϵ controls the intensity of the nonlinearity, $\delta \in [0, 1]$ is the parameter controlling the amount of dissipation, and $\gamma \neq 0$ is a free parameter leading to the recovery of a number of different dynamical systems. In particular, we perform a thorough, i.e., high definition, study of the parameter plane $\epsilon\delta$, which in fact shows very rich complex structures that we analyze in detail. Moreover,

we report and discuss the existence of novel complex sets: streets with the same periodicity and the period-adding of spring-areas. We stress that map (1) reproduces several known two-dimensional dissipative nonlinear mappings. Though, in our investigation we consider different values of γ, here we concentrate on the representative case $\gamma = -1$.

I. INTRODUCTION

The investigation of nonlinear mappings is a growing research field since the mappings may have direct applications to the understanding and characterization of many dynamical systems.

Applications range from rather different areas including biology, chemistry, social networks, mathematics, astronomy, physics, and many others. Among the set of properties present in mappings, a special characteristic is that they manifest analogous dynamical phenomena as those observed in flows with the advantage of avoiding the numerical integration of nonlinear differential equations.

To stress the richness of the multi-representative family of the dissipative nonlinear map (1), we list the following relevant cases. When $\delta = 1$ map (1) becomes conservative; in this case, several relevant studies were already done.[2,3] When $\gamma = -1$, the Fermi-Ulam model, an accelerator model where a particle is confined to bounce between two hard walls suffering elastic collisions is recovered from map (1). In this case, the variable I represents the velocity of the particle and θ denotes the phase of the oscillating wall.[4,5] Also, a periodically corrugated waveguide system can be described by map (1) with $\gamma = -1$.[6,7] This waveguide model describes the dynamics of a light ray being reflected by two corrugated surfaces. Here, the variable I corresponds to the light position, while θ denotes the angle between the incident and the reflected light. When $\gamma = 1$, mapping (1) represents the dissipative bouncer model that describes the motion of a classical particle bouncing elastically from a periodically time-varying wall in the presence of a constant gravitational field.[8] The celebrated Taylor-Chirikov's map,[9] known for describing the dynamics of a system perturbed by a sequence of pulses, can also be obtained if $\gamma = 1$ in map (1). For $\gamma = -3/2$, map (1) describes the orbital of comets due to the periodic motion of Jupiter.[10]

It is relevant to mention that an important achievement in the understanding of map (1) was made for $\delta = 1$ and $\gamma < 0$ by means of a scaling formalism.[3] In particular, it was demonstrated that the variable θ_{n+1} is uncorrelated with θ_n in the limit of vanishing I. Such a property leads to diffusion in the variable I, observed along the chaotic sea in the phase space. Moreover, in the limit of small I, such diffusion is described by a power law, in the discrete time n, of the type $I_{rms}(n) \propto (n\epsilon^2)^\beta$ with $\beta \cong 1/2$ being the acceleration exponent. From the statistical mechanics point of view, the exponent $\beta = 1/2$ makes the chaotic dynamics of the map to exhibit similar properties to that of a random walk particle, therefore leading to normal diffusion. However, the diffusion is not unlimited since the term I^γ in the second equation of map (1) decreases with the increase of I therefore producing correlations between θ_{n+1} and θ_n. Such correlations bring regularity to the phase space allowing both the existence of stable periodic orbits, generally surrounded by a periodic island of elliptical shape, and invariant spanning curves in the phase space. Such curves play a crucial role in the dynamics of the map since they limit the diffusion of chaotic orbits in the phase space and allow for a description of the dynamics in the form of scaling laws. In fact, due to the similarity of map (1) and Taylor-Chirikov's map near the transition from local to global chaos, it is possible to calculate the position of the invariant spanning curves. Indeed, their position are given, within a first order approximation, by the expression $I_{fisc} \approx \pm \epsilon^{1/(\gamma+1)}$. These two barriers, one positive and other negative, dictate the main properties of the diffusion along the chaotic sea. Starting from low values of I, an ensemble of particles diffuses with normal diffusion until reaching a regime of saturation given by $I_{sat} \propto \epsilon^\alpha$. The saturation exponent is then $\alpha = 1/(\gamma + 1)$, while the changeover from growth to the saturation is given by $n_x \propto \epsilon^z$, where $z = \alpha/\beta - 2 = -2\gamma/(\gamma + 1)$.

Regardless of the great difference, from the physics point of view, among the systems listed above all can be represented by mapping (1); therefore, the investigation of the dynamical properties of this family of mappings emerges naturally. Approaching to a more realistic situation, part of this research was carried out in the phase space for the dissipative case ($\delta \neq 1$).[1] There, the behavior of the average action at the chaotic attractors was studied and showed that dissipation destroys the different universality classes observed in the nondissipative case leading the dynamics to fall into a single set of critical exponents. For $\gamma > 0$, the relevant scaling laws are given as $I_{rms} \propto (n\epsilon^2)^\beta$, $I_{sat} \propto (1-\delta)^{\alpha_1}\epsilon^{\alpha_2}$, and $n_x \propto (1-\delta)^{z_1}\epsilon^{z_2}$, where n_x marks the changeover time from the power law growth of I_{rms} to the saturation. The exponents obtained in Ref. 1 are $\beta = 1/2$, $\alpha_1 = -1/2$, $z_1 = -1$, $\alpha_2 = 1$, and $z_2 = 2$ confirming that all are independent on the numerical values of γ.

Therefore, now in the present work, we focus on the parameter space. The question here is not about the difference between the conservative and nonconservative cases, since they are trivially different due to the arising of attractors. Our goal is to recognize domains of chaoticity and periodicity in the parameter space that have been largely reported in numerical,[11-24] experimental,[25-28] and theoretical[29-36] studies (see also references therein) after the seminal work of Fraser and Kapral.[37] Such a study does not display only the best parameters for a certain application, multistability, and cascade of periodicity domains, but can expose several dynamical features of a given system as the presence of high stability and homoclinic cubic tangencies as well as tangent, period-doubling, pitchfork, and saddle-focus homoclinic bifurcations without diving into complicated analytical methods. In this context, Lyapunov exponent λ becomes a very useful tool to investigate the attractor [periodic ($\lambda < 0$) and chaotic ($\lambda > 0$)] properties: the larger the λ value, the larger the sensibility to the initial conditions. We also determine diagrams of periodicity to identify other phenomena with respect to the period evolution under parameter changes as cascades of period-adding and period-doubling.

This paper is organized as follows. In Sec. II, we study the parameter space describing the organization of regular regions using both the Lyapunov exponent and the period of the orbits. A cusp bifurcation is observed and characterized. Moreover, a basin of attraction is obtained for a set of two different attractors near a cusp bifurcation. Section III is devoted to present our final discussion.

II. PARAMETER SPACE

In this section, we present and discuss our numerical results. For the conservative case, it is well known that the structure of the phase space is mixed; i.e., it is composed by a large chaotic sea, limited by invariant spanning curves, surrounding periodic islands (see Refs. 1–3). However, when dissipation is taken into account, the mixed structure present in the phase space for the nondissipative case is destroyed. Depending on the range of the control parameters, chaotic seas may turn into chaotic attractors while elliptical fixed points turn into sinks, i.e., attracting fixed points (see Refs. 1 and 38). To explore the influence of the dissipation in the parameter space δ vs ϵ, we use two techniques: (i) calculation of the maximum Lyapunov exponent and (ii) computation of periods. While in the latter, the period is directly computed by counting the number of points
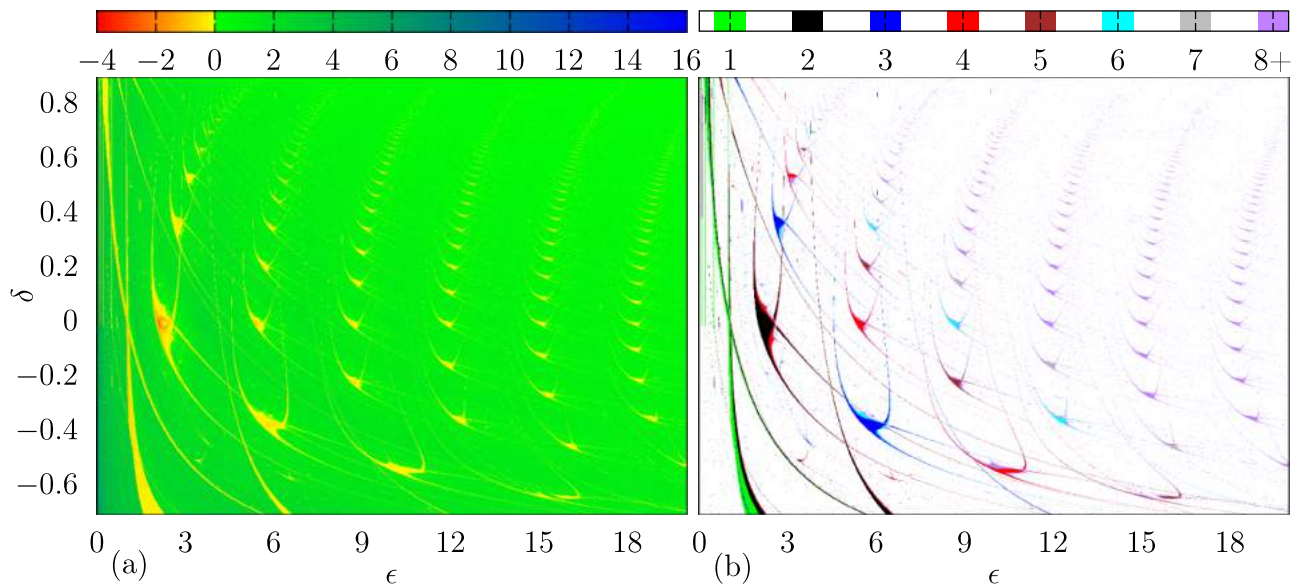
FIG. 1. Plot of the parameter space δ vs ϵ for $\gamma = -1$. The color palette indicates the maximum Lyapunov exponent in (a) while in (b) the diagram separates periodic (colored regions) from the chaotic (white regions) dynamics.
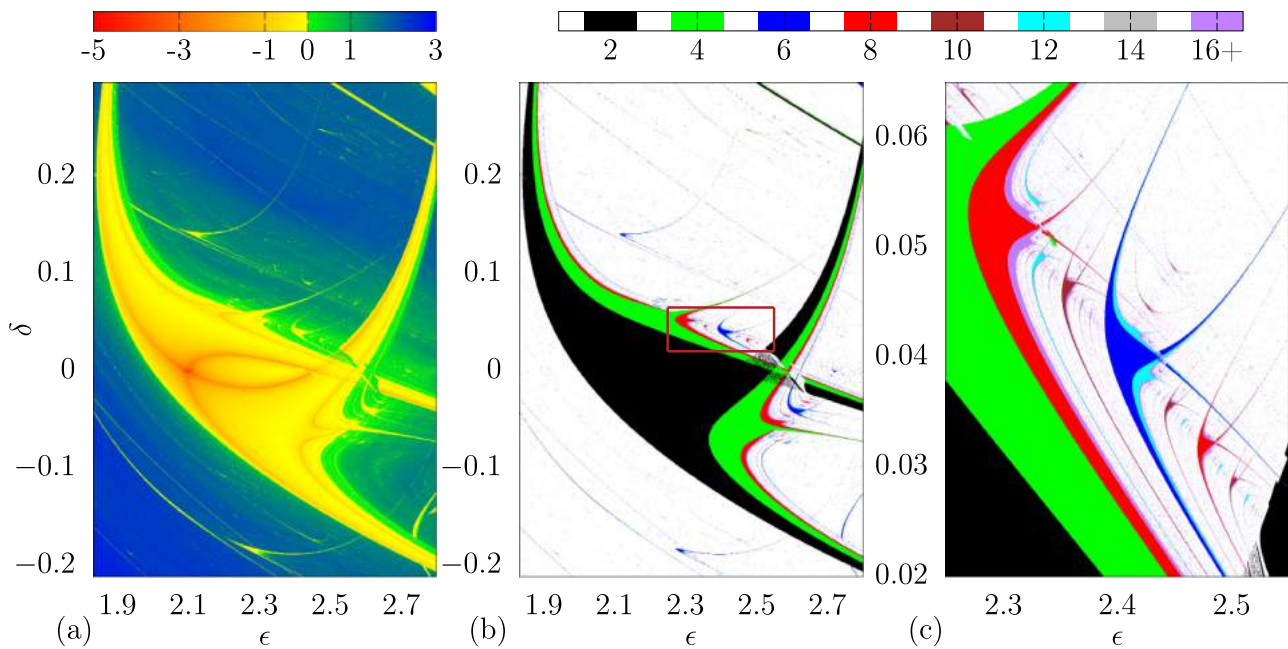

FIG. 2. (a) Amplification of a complex set from Fig. 1(a) colored according to the maximum Lyapunov exponent and (b) its corresponding domain plotted by the period of the orbits. (c) Zoom-in of the red rectangle in (b) confirming the complexity of the structure.

that compose the attractor, for (i) we compute the largest Lyapunov exponent as[39]

$$\lambda_j = \lim_{n \to \infty} \frac{1}{n} \ln \left| \Lambda_j^{(n)} \right|, \quad j = 1, 2, \ldots, \qquad (2)$$

where $\Lambda_j^{(n)}$ are the eigenvalues of the matrix $M = \Pi_{i=1}^n J_i(\theta, I)$ and J_i is the Jacobian matrix of the mapping evaluated along the orbit (θ_i, I_i). If at least one λ_j is positive, then the system is within a chaotic regime. On the other hand, when trajectories are describing periodic oscillations, all λ_j are negative. $\lambda = 0$ indicates the attractor is undergoing a bifurcation.

In our investigation, we vary δ vs ϵ for different values of γ. But, since surprisingly we observed similar results, we decided to report here $(\delta, \epsilon, \gamma = -1)$ as a representative setting of the family of solutions. We emphasize that for the case in which we focus here (i.e., $\gamma = -1$), the modulus in the first equation in (1) is not mandatory; however, for the family of maps of (1) to be valid for any $\gamma < 0$, the modulus is indispensable so that I_{n+1}^γ in the second equation can be computed. In our simulations, we favor the method of following the attractor. It means that for a given set of parameters $(\delta, \epsilon, \gamma = -1)$, the last position of the trajectory in its corresponding attractor was used as initial condition for the next neighbor set of parameters. For non-neighbor parameter sets, we consider $\theta_0 = I_0 = 0.4$ as the initial condition. The first 2×10^5 iterations were assumed as transient therefore being disregarded in all simulations. Larger transient times were tested leading to similar results. In all cases, we consider 10^3 different combinations of δ and ϵ resulting in a high resolution grid of 10^6 points in each picture.

Figure 1(a) shows a panoramic view of the parameter space for mapping (1) colored according to the maximum Lyapunov exponent. Periodic $(\lambda < 0)$ and chaotic $(\lambda > 0)$ regimes are highlighted using, respectively, red to yellow and green to blue color scales. In Fig. 1(b), the color palette refers to the orbit behavior: periodic orbits are indicated by colors (the purple corresponds to periods equal or greater than 8) and chaotic orbits are in white. As one can see, there is a large number of complex domains with periodicity following well defined patterns. Indeed, six streets are formed with domains that decrease in size and increase in period when δ grows. Additionally, the periodicity of all streets presents the period-adding phenomenon,[40] where the difference between the period P of consecutive sets in the street is always the same constant: $P_{n+1} - P_n = 1$, in the present case.

As one can see from Fig. 1, there are several different domains of periodicity, each one giving particular information about the dynamics of the system. We start to explore the dynamical properties of map (1) with the structure shown in Fig. 2.

In the periodicity region, the two red curves shown in Fig. 2(a) correspond to the high stability of the periodic attractor. It means that trajectories converge very fast to attractors along these curves. In Fig. 2(b), the boundary between the black and white regions is due to a tangent bifurcation, while the boundary between the black and green regions is a period-doubling bifurcation as so the next (between the green and red regions) and the following boundaries composing a two-dimensional Feigenbaum scenario,[41] the route to chaos via cascade of period-doubling bifurcation. This particular bifurcation composition forms a structure well studied in the early 1980s, being first discovered by Fraser and Kapral.[37] They named

this structure as fishhook but one can find it with different names in the literature, for instance, swallow,[12] crossroad area,[32] shrimp,[15] and more recently as compound window.[33] Despite those works, it is not an easy task defining precisely this periodicity set. For a discussion about it, we refer the reader to Ref. 22. Here, the dynamical system we are considering develops very similar sets of periodicity than the one shown in Fig. 2; nevertheless, they do not fit within any previous definition given its smooth transformation; see Fig. 3.

The complexity of this structure is not restricted to the continuous region of periodicity described before. The chaos due to the Feigenbaum scenario also has interesting properties. According to Fig. 2(a), it presents low sensibility to the initial conditions (green region) that contrast with the embedded high sensibility chaotic region (blue). In addition, it is also the background for a large number of cascades of self-similar sets of the main periodicity as shown in Fig. 2(c). Getting deeper into those self-similar sets, note that the biggest one has a period three times the period P of the main set of periodicity: $(3 \times P)$. And, from it, departs a period-adding cascade characterized by the constant P. For example, here the main set has period 2. In fact, in Fig. 2(c), the biggest self-similar set has period 6 and starts the period-adding with periods $(3 \times 2) \to (4 \times 2) \to (5 \times 2) \to \cdots \to (k \times 2) \ldots$, clearly characterized by the constant 2, the period of the main set. Generically, we name all this scenario (i.e., the main continuous periodicity set and its corresponding chaotic set) as *complex set*.

Another important characteristic of the complex set is the codimension-two cusp bifurcation where, from there, two curves of the tangent bifurcation depart. Each different region of periodicity has a cusp bifurcation being a remarkable bifurcation structure. The cusp bifurcation is shown in Fig. 4(a). For that simulation, we used a set of random initial conditions so that they produced a not well defined shallow region where the two periodic orbits coexist. The upper and lower boundaries of this region are tangent bifurcations that lie at the cusp bifurcation on the left side of the
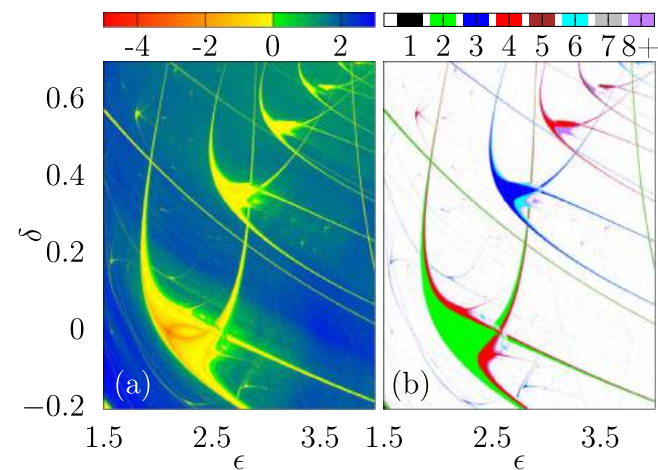

FIG. 3. (a) Plot of sequence of slightly different complex sets colored according to the maximum Lyapunov exponent and (b) the corresponding period of the orbits.
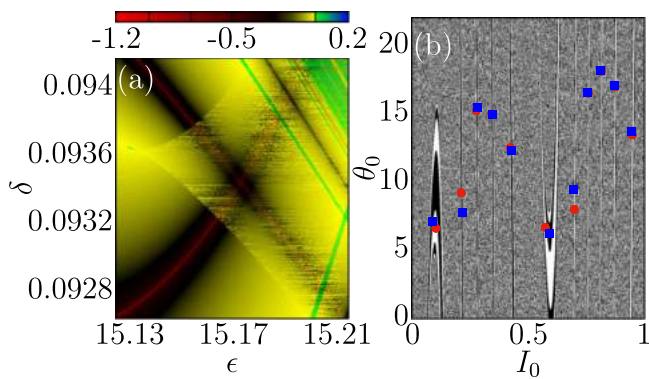
FIG. 4. (a) Magnification of a complex structure present in Fig. 2(a) to confirm a cusp bifurcation. (b) Basin of attraction: Initial conditions in the white (black) region converge to the red (blue) periodic attractor.

FIG. 6. Plot of the structures resulting from cubic homoclinic tangencies colored by the Lyapunov exponent: (a) spring-area and (b) saddle-area.

picture. In this case, the cusp bifurcation corresponds to a super-critical pitchfork bifurcation, a stable fixed point become unstable giving rise to two new stable ones. The basin of attraction of the coexisting orbits is shown in Fig. 4(b) for the parameter set $(\epsilon, \delta) = (15.1728, 0.093\,436\,5)$, the place where the two highly stable curves (in red) intersect each other.

An interesting result is also found when analyzing the interval $0 < \epsilon < 1$. As one can see in Fig. 5(a), there is a street of complex sets centered at $\delta = 0$ with an accumulation point at $\epsilon \to 0$. Moreover, Fig. 5(b) shows that the periodicity of the complex sets is the same: all have period 2. This fact is quite surprising since, in general, it is observed that in sequences of complex sets, such as in cascades and period-adding phenomena, the smaller the size of the complex set the greater the period.[17] This street breaks that idea.

Now in Fig. 6, we present two different sets of periodicity. In contrast to the complex set, it was rigorously demonstrated by Gonchenko et al.[30,42] that they come from a cubic homoclinic tangency; i.e., an orbit composed by cubic tangencies between the
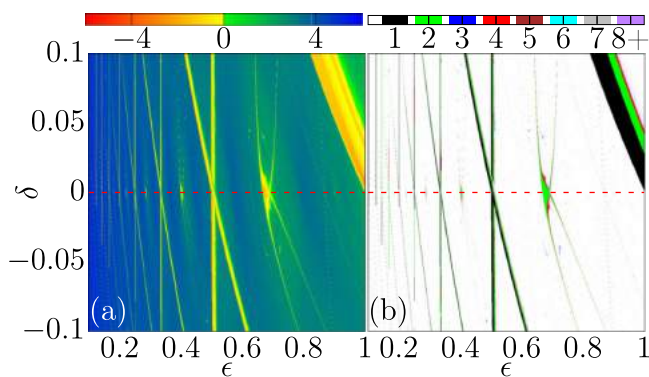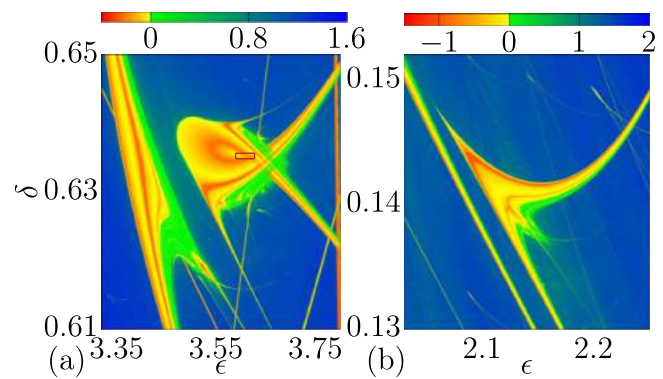
stable and unstable manifolds of a fixed point x_0, thereafter the orbit converges to the fixed point for positive and negative iterations: $x_n \to x_0$ for $n \to \pm\infty$. This structure occurs whenever near the fixed point the dynamics can be described by a cubic dynamical system. If the cubic term is negative, there is a spring-area structure, as shown in Fig. 6(a). If it is positive, the structure is the saddle-area presented in Fig. 6(b). For more details about the theory, we recommend the reader to refer to Ref. 42.

Indeed, we want to remark that in Ref. 42, analogous universal windows of stability were found, i.e., cascades of spring and saddle-areas, in two-dimensional separatrix maps. Also, there, the role of cubic and double quadratic homoclinic tangencies in the formation of such structures was clarified and thoroughly described.

The spring and saddle-areas are also composed by regions of periodic and chaotic behavior. The scenario presented in the chaotic region of the complex set composed by cascades of self-similar complex sets and period-adding organization is also observed in the chaotic region of these structures. The difference starts with the
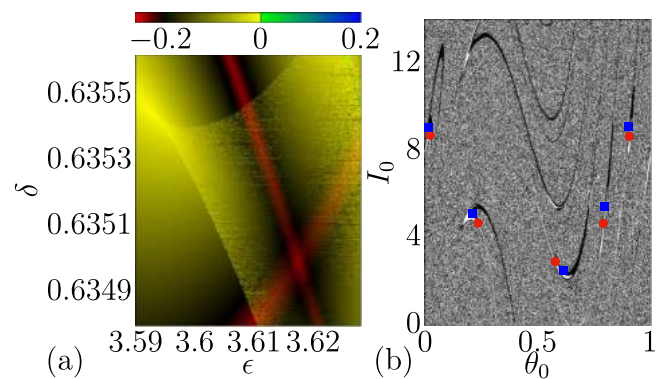

FIG. 5. (a) Confirmation of the symmetry of the structures living in the parameter space δ vs ϵ with respect to $\delta = 0$. In (b), the same symmetry viewed in the period of the orbits present in the stability regions.

FIG. 7. (a) Magnification of the region delimited by a rectangle in Fig. 6(a). (b) Basin of attraction for the parameter set $(\epsilon, \delta) = (3.617\,44, 0.634\,989)$; the place where the two high stable curves (red) intersect each other. Initial conditions in the white (black) region converge to the red (blue) periodic attractor.
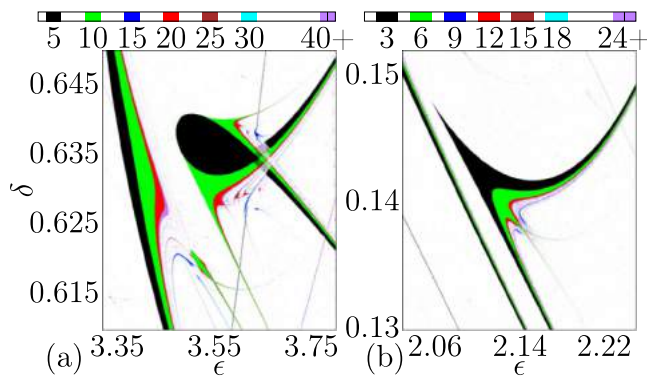
FIG. 8. Plot of the structures resulting from cubic homoclinic tangencies (periodicity): (a) spring-area and (b) saddle-area. Compare with Fig. 6.

curves of high stability. In the complex set, there are two such curves intersecting once. In the spring-area, there is just one curve intersecting itself once (see the coexisting attractors and the cusp bifurcation in Fig. 7), and finally, in the saddle-area, there is also one curve of high stability with no intersection.

According to the periodicity, the Feigenbaum scenario is also presented in both spring and saddle-areas, but the boundaries between the main bodies of periodicity with the chaotic regions are different. Let us consider the way from the chaotic region to the main body composed by the fixed point in Fig. 8 (for instance, a period P orbit is a fixed point when considering intervals of P iterations). In the spring-area [Fig. 8(a)], the boundary is caused by a subcritical period-doubling bifurcation: an unstable fixed point in the white region becomes stable and gives rise to an unstable period two orbit in the black region. In the case of the saddle-area [Fig. 8(b)], the boundary is formed by two tangent bifurcations that met at a subcritical pitchfork bifurcation; here, the unstable fixed point becomes stable giving rise to two new unstable fixed points.
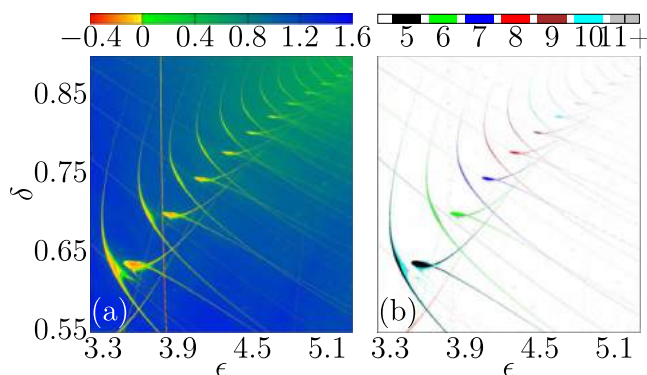

FIG. 9. Plot of the parameter space δ vs ϵ highlighting part of a street shown in Fig. 1(a) colored by the Lyapunov exponent while in (b) the color identifies the period of the structure.

As a final result, we present in Fig. 9 a street of spring-areas organized by period-adding; even though the theory predicts cascades of spring and saddle-areas.[42] As far as we know, period-adding in these structures was never reported before; therefore, we confirm the first evidence of such structure in the family of two-dimensional mappings described by Eq. (1).

III. FINAL REMARKS AND CONCLUSIONS

We have characterized the mapping of Eq. (1) that reproduces several known two-dimensional dissipative nonlinear mappings. By observing structures of periodicity in the high definition parameter space, we identified several dynamical features in the system. Tangent, period-doubling, pitchfork, and cusp bifurcations were found and discussed in detail so as cascades of period-adding, period-doubling, and the Feigeinbaum scenario. We also conclude that both cubic homoclinic tangencies are present in the system due to the existence of spring and saddle-area structures. Moreover, we showed novelties that could potentially give insights into new theoretical concepts, as the definition of the complex sets, streets with the same periodicity, and the period-adding of spring-areas. Our analysis, even deep in nonlinear dynamical theory, is not based on analytical approaches, most often available only to specialists. Instead, we consider a very simple method based on detailed simulations of the parameter space.

We hope that our work could be useful for both: as an example of characterization and description of the structure of periodicity sets and as a motivation for researchers dealing with deep analytical formalisms.

REFERENCES

[1] J. A. de Oliveira and E. D. Leonel, J. Phys. A **45**, 165101 (2012).
[2] J. A. de Oliveira, R. A. Bizão, and E. D. Leonel, Phys. Rev. E **81**, 046212 (2010).
[3] E. D. Leonel, J. Penalva, R. M. N. Teixeira, R. N. Costa Filho, M. R. Silva, and J. A. de Oliveira, Phys. Lett. A **379**, 1808 (2015).
[4] M. A. Lieberman and A. J. Lichtenberg, Phys. Rev. A **5**, 1852 (1971).
[5] E. D. Leonel, P. V. E. McClintock, and J. K. L. da Silva, Phys. Rev. Lett. **93**, 014101 (2004).
[6] E. D. Leonel, Phys. Rev. Lett. **98**, 114102 (2007).
[7] G. A. Luna-Acosta, J. A. Mendez-Bermudez, and F. M. Izrailev, Phys. Rev. E **64**, 036206 (2001); Phys. Lett. A **274**, 192 (2000).
[8] L. D. Pustylnikov, Trans. Moscow Math. Soc. **2**, 1 (1978).
[9] B. V. Chirikov, Phys. Rep. **52**, 263 (1979).
[10] G. M. Zaslavsky, *Hamiltonian Chaos and Fractional Dynamics* (Oxford University Press, Oxford, 2005).

[11] J. Rössler, M. Kiwi, B. Hess, and M. Markus, Phys. Rev. A **39**, 5954 (1989).

[12] M. Markus and B. Hess, Comput. Graph. **13**, 553 (1989).

[13] M. Komuro, R. Tokunaga, T. Matsumoto, L. O. Chua, and A. Hotta, Int. J. Bifurcat. Chaos **1**, 139 (1991).

[14] A. P. Kuznetsov, S. P. Kuznetsov, I. R. Staev, and L. O. Chua, Int. J. Bifurcat. Chaos **3**, 943 (1993).

[15] J. A. C. Gallas, Phys. Rev. Lett. **70**, 2714 (1993).

[16] L. Glass, Nature **410**, 277 (2001).

[17] S. L. T. de Souza, A. A. Lima, I. L. Caldas, R. O. Medrano-T, and Z. O. Guimarães-Filho, Phys. Lett. A **376**, 1290 (2012).

[18] P. C. Rech, Eur. Phys. J. B **86**, 356 (2013).

[19] F. Hegedüs, Ultrasonics **54**, 1113 (2014).

[20] R. O. Medrano-T and R. Rocha, Int. J. Bifurcat. Chaos **24**, 1430025 (2014).

[21] D. V. Savin, A. P. Kuznetsov, A. V. Savin, and U. Feudel, Phys. Rev. E **91**, 062905 (2015).

[22] A. C. C. Horstmann, H. A. Albuquerque, and C. Manchein, Eur. Phys. J. B **90**, 96 (2017).

[23] K. Klapcsik and F. Hegedüs, Chaos Solitons Fractals **104**, 198 (2017).

[24] F. Hegedüs, W. Lauterborn, U. Parlitz, and R. Mettin, Nonlinear Dyn. **94**(1), 273–293 (2018).

[25] O. Feo and G. M. Maggio, Int. J. Bifurcat. Chaos **13**, 2917 (2003).

[26] D. M. Maranhão, M. S. Baptista, J. C. Sartorelli, and I. L. Caldas, Phys. Rev. E **77**, 037202 (2008).

[27] R. Stoop, P. Benner, and Y. Uwate, Phys. Rev. Lett. **105**, 074102 (2010).

[28] D. W. C. Marcondes, G. F. Comassetto, B. G. Pedro, J. C. C. Vieira, A. Hoff, F. Prebianca, C. Manchein, and H. A. Albuquerque, Int. J. Bifurcat. Chaos **27**, 1750175 (2017).

[29] P. Gaspard, R. Kapral, and G. Nicolis, J. Stat. Phys. **35**, 697 (1984).

[30] S. V. Gonchenko, Selecta Mathematica Sovietica **10**, 69 (1991) (Translated from Methods of Qualitative Theory of Differential Equations; Gorky State University, 1985, 55–72).

[31] C. Mira, *Chaotic Dynamics* (World Scientific, Singapore, 1987).

[32] J. P. Carcassés, C. Mira, M. Bosch, C. Simó, and J. C. Tatjer, Int. J. Bifurcat. Chaos **1**, 183 (1991).

[33] E. N. Lorenz, Physica D **237**, 1689 (2008).

[34] R. Barrio, F. Blesa, and S. Serrano, Phys. Rev. Lett. **108**, 214102 (2012).

[35] E. S. Medeiros, R. O. Medrano-T, I. L. Caldas, and S. L. T. de Souza, Phys. Lett. A **377**, 628 (2013).

[36] D. R. da Costa, M. Hansen, E. D. L. G. Guarise, and R. O. Medrano-T, Phys. Lett. A **380**, 1610 (2016).

[37] S. Fraser and R. Kapral, Phys. Rev. A **25**, 3223 (1982).

[38] C. M. Kuwana, J. A. de Oliveira, and E. D. Leonel, Physica A **395**, 458 (2014).

[39] J. P. Eckmann and D. Rulle, Rev. Mod. Phys. **57**, 617 (1985).

[40] K. Kaneko, Progr. Theoret. Phys. **68**, 669 (1982).

[41] M. J. Feigenbaum, Los Alamos Science **1**, 4 (1980).

[42] S. V. Gonchenko, C. Simó, and A. Vieiro, Nonlinearity **26**, 621 (2013).